PREPRINTS

of the

STEWARD OBSERVATORY

THE UNIVERSITY OF ARIZONA
TUCSON, ARIZONA 85721 U.S.A.

No. 1201
C94/02/16

PROPERTIES OF OBJECTS NEAR THE MAIN SEQUENCE EDGE

Adam Burrows
Departments of Physics and Astronomy
University of Arizona
Tucson, Arizona 85721

and

W. B. Hubbard, J. I. Lunine, and D. Saumon
Department of Planetary Sciences
University of Arizona
Tucson, Arizona 85721

To be published by World Scientific
in the Proceedings of the International Conference on
"Critique of the Sources of Dark Matter in the Universe"
ed. David B. Cline
held in Los Angeles, California, February 16-18, 1994

Arizona Theoretical Astrophysics Preprint #94-16

PROPERTIES OF OBJECTS NEAR THE MAIN SEQUENCE EDGE

A. BURROWS
Departments of Physics and Astronomy, University of Arizona
Tucson, Arizona 85721, USA

and

W. B. HUBBARD, J. I. LUNINE, AND D. SAUMON*
Department of Planetary Sciences, University of Arizona
Tucson, Arizona 85721, USA

ABSTRACT

The search for dim red/infrared stars and substellar objects is experiencing a renaissance, fuelled in part by recent advances in infrared technology. Dim stars less massive than $0.5M_\odot$ could represent more than two-thirds by number and more than 50% by mass of all stars in the galactic disk and bulge. Furthermore, the recent MACHO detections imply that brown dwarfs may constitute a significant fraction of the galactic halo. This observational activity requires for its interpretation a comprehensive theory of dM stars and substellar brown dwarfs. All issues concerning mass functions, the temperature scale of M dwarfs, the stellar content of the galactic disk, bulge, and halo, the halo emissions of other galaxies, and the subdwarf population of our galaxy hinge on substantially improving our theoretical understanding of dim objects near the main sequence edge. In this paper, we discuss some of the current issues in modeling M dwarfs and brown dwarfs.

1. Introduction

Spanning more than an order of magnitude in mass, the late M and brown dwarf branches are still all but unexplored. However, stars less massive than $0.5M_\odot$ must represent more than two-thirds by number and perhaps more than 50% by mass of all stars in the galactic disk.[1,2] Despite their manifest importance, such M dwarfs have only recently received commensurate observational and theoretical attention. With the growth and steady improvement of infrared astronomical technology (HgCdTe and InSb arrays, cryostats, speckle, etc.), the search for dim stars and substellar objects (brown dwarfs) has accelerated. As a result, the list of individual candidate brown dwarfs has swollen beyond twenty (Table 1). Brown dwarfs straddle the realms of planets and stars, are made predominantly of liquid metallic hydrogen, have atmospheres of molecules and grains, and can achieve central

* Hubble Fellow

temperatures adequate to consume their stores of cosmological deuterium, while inadequate to ignite sufficient light hydrogen to avoid cooling into obscurity within a Hubble time. Nevertheless, they are characterized by straightforward extrapolations of the same equation-of-state (EOS) and atmospheric physics appropriate for the more massive M dwarfs. Brown dwarfs and M dwarfs must be studied together as part of a continuum.

Table 1
Brown Dwarf Candidates and Lowest-Luminosity *M* Dwarfs.[a]

Name	K	J−K	M_K	Mass ($M_\odot$)	Spectral Type
(a) Field stars and very wide binary companions					
GD165B	14.09	1.66	11.78	-	>M9
LHS2065	10.75	1.34	10.31	-	M9
LHS2924	10.68	1.24	10.48	-	M9
GL569B	9.65	1.13	9.55	-	M8.5
PC0025+0447	14.93:	-	-	-	M9.5
(b) Unresolved companions					
G29-38B?	13.45	-	12.70	-	-
HD114762B	-	-	-	>0.011	-
(c) Companions with astrometric mass determinations					
G208-44B	8.28	1.06	10.00	0.087 ± 0.014	-
GL623B	8.85	1.13	9.46	0.079 ± 0.010	-
LHS1047B	8.04	1.01	9.42	0.057 ± 0.079	-
Ross 614B	7.24	1.09	9.17	0.085 ± 0.030	-
(d) From Tinney *et al.* 1993:					
TVLM 868-110639	11.44	1.28			
TVLM 513-46546	10.77	1.19			
TVLM 513-8328	13.03	1.14			
BRI 0021-0214	10.64	1.26			
(e) Clusters:					
ρ Oph: 7 Objects (Comeron *et al.* 1993)					
Pleiades: 3 Objects (Stauffer *et al.* 1989)					

[a] Data taken from Henry (1991),[3] Kirkpatrick, Henry, and McCarthy (1991),[4] Latham *et al.* (1989),[5] Schneider *et al.* (1991),[6] Becklin and Zuckerman (1988),[7] Tinney, Mould, and Ried (1993),[8] Comeron *et al.* (1993),[9] and Stauffer *et al.* (1989).[10] Table adapted from Burrows and Liebert (1993).[11]

2. Stellar Modeling

Since the fortuitous false start of VB8B and in parallel with the observational explosion, the theoretical studies of late M dwarfs and brown dwarfs have improved in sophistication.[12,13,14,15,16,17,18,19,20,21] Importantly, new theoretical spectral syntheses are being published[22,23,24,25] that in principle can be compared directly with the

IR photometry and spectrophotometry accumulating in the literature (e.g. Kirkpatrick *et al.*;[26] Tinney *et al.*[8]) to extract such physical parameters as gravities, metallicities, effective temperatures, and masses.

Though the old theory of M dwarfs and low-mass stars ($\lesssim 0.7 M_\odot$) has a long pedigree[27,28,29] it has been successful in detail only above 0.3 $M_\odot$. Below 0.3 $M_\odot$, the inferred radii and effective temperatures (T_e) in particular have been problematic and an acceptable fit to the observational H-R diagram has been elusive. An adequate theory must incorporate (1) a good equation of state (EOS) from the molecular hydrogen phase, through the molecular dissociation and ionization regions, to the metallic H/He region; (2) a detailed treatment of the atmospheric opacities for T_e below 3500 K and gravities in the 10^5 cm s^{-2} range; and (3) nuclear rates suited to the "low" ($< 7 \times 10^6$ K) central temperature (T_c), high central density (2000 g cm^{-3} $> \rho_c >$ 100 g cm^{-3}) regimes encountered along the M dwarf/brown dwarf continuum.

2.1. The Equation-of-State and Thermodynamics of Dense H/He Mixtures

More than 50 years ago, Wigner and Huntington[30] postulated that under high pressures molecular hydrogen would undergo a phase transition to the metallic state. This metal-insulator transition is now the subject of an intense, but still ambiguous, experimental quest.[31,32,33] Nevertheless, the metallization of hydrogen and hydrogen/helium mixtures is unavoidable given suitable pressure ($P \gtrsim 3$ Mbars) and such an alloy must comprise the bulk of Jupiter (~85%), Saturn (~50%), brown dwarfs (>99.9%), and late M dwarfs. Theoretical treatments of the thermodynamics of such strongly-coupled Coulomb plasmas in astrophysical contexts have been attempted by many.[34,35,36,37,38,39,40,41,42,43] SC[43] in particular have provided a most careful theoretical treatment of pure hydrogen above and below the plasma phase transition (PPT), at high and low temperatures, and in the molecular, atomic, and ionized state. A revealing temperature-density phase diagram for pure hydrogen inspired by SC and Saumon[44] is shown in Figure 1, taken from Burrows and Liebert.[11] This figure depicts most of the essential information concerning the thermodynamics of the entire brown dwarf and giant planet family. A Jupiter (J) and two 0.05 $M_\odot$ brown dwarf adiabats are shown on Fig. 1 as dotted lines. Note that, though these adiabats assume a helium mass fraction (Y_α) of 25% (for the dwarf) and 22% (for Jupiter), their superposition on a pure hydrogen phase diagram still makes for a fruitful comparison. The X's on these lines mark the points interior to which lie 50% of the object's mass. As is apparent, only a small fraction of the mass of these objects inhabits the low-temperature, low-density regime while most of their mass is indeed in the liquid metallic state.

As part of a continuing effort to improve the description of the interiors of very low mass stars and brown dwarfs, we have recently compared the Marley and Hubbard (MH) equation of state, which we used in our previous interior models, with the recently available SC EOS. The latter EOS represents the latest effort to account for the complex non-ideal behavior of hydrogen in the interior of cool stars,

in particular in the regime of *pressure ionization* ($\rho \approx 1$ g/cm^3) where it naturally predicts a *first-order phase transition* around pressures of 1 Mbar, with a critical point located at T_c =15300 K and P_c =0.614 Mbar (the PPT). The PPT separates a mostly molecular, low-density phase and a partially ionized ($\approx 50\%$), high-density metallic phase. Most of a brown dwarf and most of objects near the main sequence edge can be found on the top right-hand-side of Figure 1 in the high-density, liquid metallic region.

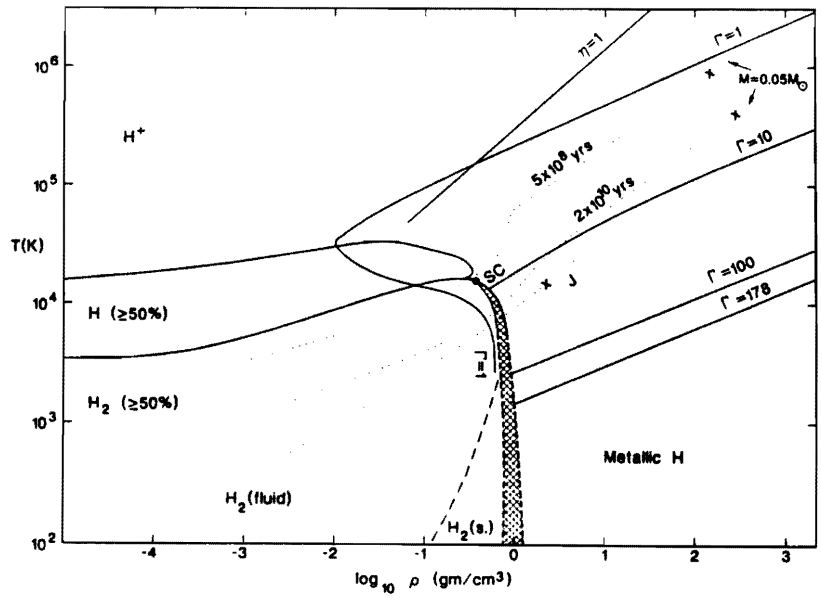

Figure 1. Phase diagram of temperature (in K) vs density (in g/cm^3) for pure hydrogen. Superposed as dotted curves are two $0.05M_\odot$, Y_a =0.25 brown dwarf adiabats from BHL at 5×10^8 and 2×10^{10} yr and a Jupiter (J) adiabat. The ×'s on these adiabats mark the 50% mass point. Lines of constant Coulomb parameter (Γ) are provided. Shown clockwise are the solid H_2, liquid and gaseous H_2, atomic H, ionized H^+, and metallic H states. "SC" marks the critical point as calculated in Saumon and Chabrier,[42] to which one is referred for further details. The hatched region represents schematically the realm of the first-order plasma phase transition. See Burrows and Liebert[11] for discussion.

A comparison of the MH and SC hydrogen equations of state along a series of adiabats representative of M dwarfs and brown dwarfs shows an excellent agreement in the low density fluid consisting of H atoms and H_2 molecules and in the very dense fully ionized metallic fluid. Not surprisingly, significant differences arise in the regime of pressure ionization and in the relatively low density metallic fluid where the polarizability of the electron fluid is treated differently. In this narrow density range ($-0.5 \leq \log\rho \leq 0.5$), the differences in temperature and pressure along the adiabats can be as high as 30%. The largest differences are found in the regime where temperature and pressure ionization are of comparable importance. Different treatments of the internal partition function of atomic H lead to disagreements of 50% along the relevant adiabat.

We also compared the SC EOS with other hydrogen EOS's which are widely used in astrophysical applications.[45,39,46] Overall, the SC EOS is found to be clearly superior for applications to low-mass stars, brown dwarfs and giant planets. For instance, Stringfellow uses the Eggleton, Faulkner and Flannery[47] equation of state which ignores Coulomb corrections in the dense, fully ionized regime. These corrections are important for the description of the thermal structure of both M dwarfs and brown dwarfs and will also affect the mechanical structure of young and relatively massive objects which are partially degenerate. Ignoring the Coulomb corrections to the pressure and entropy, which are negative, leads to an overestimate of the pressure and to larger radii.

2.2. Atmospheric Physics and Radiative Transfer

2.2.1. Atmospheric Composition

With effective temperatures below 3500 K, M and brown dwarfs bear a superficial resemblance to red giants and by their extreme red colors could be confused with them. However, their surface gravity is some six to seven orders of magnitude larger than that of a giant. The high gravities and the similar or lower effective temperatures imply that brown dwarf and M dwarf photospheric pressures and densities exceed those of giants by a similar factor. Therefore, the atmosphere, instead of being dominated by atomic species, is comprised mostly of molecules. Furthermore, below about 2400 K, grains condense out and can contribute significantly to the continuum opacity. Molecules and grains provide the distinguishing spectral features at the edge of the main sequence. In addition to the molecular hydrogen (H_2) and neutral helium that dominate the atmosphere, H^- can be found. The metals are in their neutral, singly-, and doubly-ionized states deep inside the atmosphere at 10^4 K, but near the photosphere are found as hydrides (CaH, MgH, SiH), oxides (TiO, VO), magnesium silicates (e.g. enstatite ($Mg_2Si_2O_6$)), carbides (e.g. Fe_3C), and iron grains. The C/O ratio determines the chemistry of carbon. For C/O > 1, carbon tends to be incorporated in CO and graphite grains, but for C/O < 1 and very low temperatures ($\lesssim$ 600K), it tends to be in CH_4. The abundance of Fe_3C is also regulated by the carbon abundance. Oxygen is not only incorporated in silicates and CO, but in H_2O as well. "Steam" bands play an important role in spectrum formation and may be the most useful brown dwarf signatures, centered as they are between the infrared J, H, and K bands.[48,49,50,24]

2.2.2. Opacities

With such a plethora of species to consider, the radiative transfer and spectral synthesis calculations are formidable. However, the molecular features in M dwarf and brown dwarf spectra provide essential and critical diagnostics that must be mastered before cool stars and brown dwarfs are to be understood. The major opacity sources come from H^-, H_2^-, He^-, atomic hydrogen transitions, Rayleigh

scattering, bound-free transitions of Mg, Si, and Ca, the electronic bands of FeH, MgH, CaH, and SiH, the rotation-vibration transitions of TiO, H_2O, and CO, and the collisionally-induced dipole moment of H_2.[51] The latter is particularly important at low metallicities. The opacity due to grains requires special knowledge — we need the particle size spectrum ($a \sim 1$–$10\,\mu$m?), the vertical distribution of the grain "clouds," their patchiness, and their composition. Lunine *et al.*[50] made the first detailed attempt to understand cloud physics by studying grain coalescence, aggregation, and transport, and the vapor pressure curves of the relevant solids.

2.2.3. Radiative Transfer

There has in fact been real theoretical progress over the last few years in understanding the emission of cool, dense atmospheres.[22,25,24,50] Recent theoretical spectra from Allard[22] and Allard *et al.*[23] deserve special mention for their completeness and clarity. However, they do not study brown dwarf spectra ($T_e < 2000$ K), but concentrate on late M dwarfs (2000 K$< T_e <$ 3500 K). There are as yet no good theoretical models of brown dwarf spectra.

The atmosphere models that we have employed in our stellar evolution calculations over the last few years have undergone steady and systematic improvement. As described in Lunine *et al.*,[50] we had first used the standard Eddington approximation, $J = 3K$ throughout the atmosphere, where J is the mean intensity and K the second moment of the radiation field. Such an approximation is valid for an atmosphere fully in radiative equilibrium, or for one in which the convection zone begins at large optical depth (and, hence, is effectively decoupled from the radiative zone).

Convection is handled in the models using the standard mixing-length treatment, with a mixing length set equal to the pressure scale height. In a previous paper (BHL), we had studied the dependence on mixing length and determined that near one pressure scale height, the mixing length dependence is weak.

However, for brown dwarfs and M dwarfs of high effective temperature (i.e., above 2500 K) and low surface gravity, we find that the top of the convection zone is in fact at optical depths well below unity, invalidating the use of the Eddington approximation. Therefore, we now explicitly solve the transfer equation to derive the temperature profile. The radiative transfer code we now employ was modified from that of Bergeron, Wesemael & Fontaine,[52] which solves the transfer equation for a temperature-pressure profile using the Feautrier method.

2.3. Nuclear Processes

The thermonuclear processes relevant at the temperatures and densities in the stellar edge regime are

$$p + p \rightarrow d + e^+ + \nu_e, \quad \text{where} \quad Q_p = 1.442 \text{ MeV} \tag{1}$$

and

$$p + d \rightarrow {}^3\mathrm{He} + \gamma, \quad \text{where} \quad Q_d = 5.494 \text{ MeV}. \tag{2}$$

Reaction (1) is the rate-limiting process, as it proceeds by the weak interaction. The rates from these proton- and deuterium-burning reactions were obtained from Fowler, Caughlan, and Zimmerman (FCZ).[53] At the high densities ($\rho_c \sim 100 - 2000$ g cm^{-3}) and "low" temperatures ($T_c \sim [2 - 6] \times 10^6 K$) reached by M dwarfs, the Coulomb parameter, Γ ($= Z^2 e^2 / r_i k_B T$), is of order unity. Hence, the screening corrections to the thermonuclear rates on the hydrogen main sequence are not negligible ($\sim 1.1 - 2.0$), and we have used the intermediate screening algorithm of Graboske *et al.*[54] to calculate them. The temperature dependence of the corrected FCZ rate of reaction (1) in the central temperature regime of M dwarfs is strong and roughly $\propto T^{6-8}$. Pycnonuclear rates for all the densities encountered in this study are negligible.

Since T_c does not exceed $\sim 6 \times 10^6$ K for $M < 0.2 M_\odot$, ^{3}He does not accumulate rapidly. The low ^{3}He fraction and temperatures inhibit ^{3}He-burning by the processes ^{3}He(^{3}He, $2p$)^{4}He and ^{3}He(^{4}He, γ)^{7}Be of the standard $p-p$ chain. As a consequence, ^{3}He takes much longer than 20 Gyr to reach equilibrium and the $p - p$ chain is truncated. Primordial deuterium will burn at low temperatures ($\sim 5 \times 10^5$ K) by reaction (2), on a "deuterium main-sequence" phase that lasts as much as $\sim 10^7$ yr for objects more massive than $\sim 0.014 M_\odot$.

3. A Brief Synopsis of Some of Our Evolutionary Calculations

3.1. Solar Metallicity

The solid lines on Figure 2 taken from Burrows *et al.*[21] portray the evolution of the luminosity with time for objects with solar metallicity and $Y_\alpha = 0.25$ from 0.01 $M_\odot (\sim 10\ M_J)$ to 0.2 $M_\odot$. In this figure, the highest mass stars ($\sim 0.15 - 0.2\ M_\odot$) commence deuterium burning as early as $\sim 10^5$ years. All these "stars" are fully convective. Those massive enough to land on the hydrogen main sequence would stay there for at least 100 Gyr, most for far longer. For these stars, since the age of the Galaxy is no more than 20 Gyr, evolution beyond, and even on, the main sequence is slow and only of academic interest. For the brown dwarfs that do not ignite a significant amount of hydrogen during their Kelvin-Helmholtz contraction ($M \lesssim 0.06 M_\odot$), 20 Gyr is ample time for them to cool into obscurity ($T_e < 600$ K).

As is clear from Figure 2, deuterium burning is crucially important below $\sim 10^7$ years and maintains the luminosity above what would otherwise obtain without deuterium by as much as a factor of 5. Hence, for young clusters such as ρ Ophiuchus ($\sim 3 \times 10^6$ years) and Taurus-Auriga ($\sim 10^6$ yrs), deuterium burning cannot be ignored. If Y_d is increased to 5×10^{-5}, during deuterium burning the luminosities are larger by $\sim 50\%$ near the hydrogen main sequence edge.

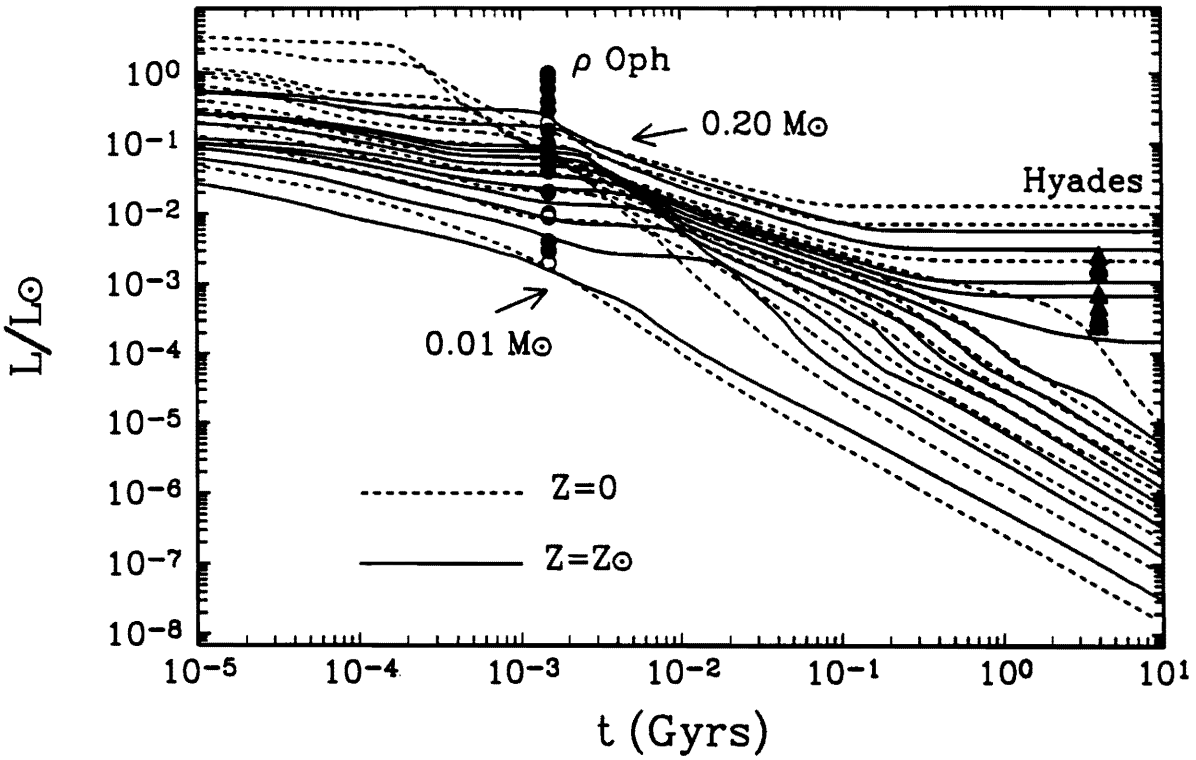

Figure 2. Curves of luminosity vs. time for 12 fixed masses: 0.01 to 0.10 $M_\odot$ in steps of 0.01 $M_\odot$, plus 0.15 and 0.20 $M_\odot$. Curves are shown for zero (dashed) and solar (solid) metallicity. Hyades data (triangles) are from Bryja *et al.*,[54] while ρ Oph data (circles) are from Comeron *et al.*.[9] Open circles denote ρ Oph objects for which only two measured magnitudes are available. The pronounced "ripple" in the middle of the curves marks the conclusion of deuterium burning, which appears later and at lower luminosities for objects of solar metallicity. A more subdued ripple at $\sim 10^{-4} L_\odot$ is due to the appearance of dust grains near the photosphere; this effect is of course only present in the objects with solar metallicity.

After deuterium burning, the luminosities continue their decay. However, hydrogen burning proper commences near 2×10^8 years for the more massive objects ($\geq 0.1\ M_\odot$) and near 10^9 years for objects near $0.07\ M_\odot$. If the star has sufficient mass ($M > M_{edge}$), its luminosity stabilizes on the hydrogen main sequence. If not, though hydrogen burning may occur for a time, it aborts and the object's luminosity continues its decay. The separation between these two branches, the M dwarfs and brown dwarfs, is clearly seen in the right of Figure 2. To resolve the edge, evolutionary calculations were performed in mass increments of at most 0.001 $M_\odot (\sim 1 M_J)$ (and, right near the edge, of $\sim 0.0001 M_\odot$) in the transition region. The edge was found to be $0.077\ M_\odot$ for solar metallicities. Note that at an age of 2×10^{10} years, the luminosity ranges an extraordinary six orders of magnitude for objects from $0.01\ M_\odot$ to $0.2\ M_\odot$.

To illustrate one of the uses of these calculations, we have superposed on Figure 2 the recent data for ρ Ophiuchus from Comeron, Rieke, Burrows, and Rieke[9] and,

for the Hyades, from Bryja *et al.*.[55] Comeron et al. report some seven substellar objects in the core of the ρ Oph stellar clouds, included among some 91 infrared sources. They use these results to derive a power-law mass function that extends into the brown dwarf region. However, it is interesting to note that unlike the results derived for M dwarfs in the Hyades by Hubbard *et al.*,[56] the Comeron study seems to penetrate into the brown dwarf mass range by virtue of the much higher luminosities of brown dwarfs in the very young ρ Oph association. As Figure 2 illustrates, despite the age ambiguity of the ρ Oph objects, if there are no significant errors in the extinction corrections and distance estimates, ρ Oph seems to be rich in brown dwarfs down to a mass of $\sim 0.01\ M_\odot$.

3.2. Zero-Metallicity

The evolution of the zero-metallicity case is homologous to that of the solar metallicity models. The dashed lines of Figure 2 depict the evolution of the luminosity with time for various masses ($0.01 M_\odot$ to $0.2 M_\odot$) and shows that $Z = 0$ models evolve faster in the sense that every phase of the evolution (deuterium burning, settling on the main sequence, split between stars and brown dwarfs) occurs much earlier than in the solar-metallicity case. This is a direct consequence of the lower atmospheric opacities. For *fixed* T_e and g, the lower κ_R forces the top of the convection zone further down into the atmosphere to higher pressures, where the specific entropy is *lower*. Since convection is very nearly adiabatic, the entropy of the interior is fixed by the P and T values at the top of the convection zone. Conversely, for models with a fixed *mass* and interior entropy (which determine the structure of a model), the $Z = 0$ model will have nearly the same radius, but a higher T_e. This results in a higher luminosity and faster evolution.

Another consequence of lower atmospheric opacities is the increase of the minimum mass for hydrogen burning on the main sequence. For models that reach a stable configuration on the main sequence, the higher luminosity of the $Z = 0$ case requires more vigorous nuclear burning to maintain the equilibrium. This can be achieved only for higher mass stars. The dependence of T_e and L at the edge of the main sequence on Z is very strong. We emphasize the importance of accurate opacities for the determination of the true location of the edge of the main sequence. The minimum mass for the $Z = 0$ main sequence obtained here, $0.092\ M_\odot$, is the lowest reported so far. It can be demonstrated analytically that the minimum main-sequence mass decreases when the atmospheric opacity is increased.[21] Using opacities which did not include the H_2 collisionally-induced term and an approximate grey surface BC, D'Antona[13] obtained a value of $0.115\ M_\odot$. With updated opacities which include the H_2 collisional term, Burrows *et al.*[21] revised this value downward to $0.094\ M_\odot$. This arises from the substantial increase in opacity due to H_2 absorption. By using nongrey atmospheres as a surface BC, which effectively increases the average atmospheric opacity compared to the otherwise identical grey case, the new value of $0.092\ M_\odot$ is obtained.

Saumon *et al.*[24] have computed an extensive grid of zero-metallicity grey atmo-

sphere models in the range $900 \leq T_e\,(\mathrm{K}) \leq 4500$ and $2.0 \leq \log g\,(\mathrm{cm/s^2}) \leq 5.5$ for helium mass fractions Y=0.22 and 0.25. This large number of models was computed mostly to provide surface boundary conditions for our evolutionary calculations. A somewhat reduced grid of nongrey models with $1500 \leq T_e \leq 5000$, and $3.5 \leq \log g \leq 5.5$ for Y=0.25 was also generated. A zero-metallicity spectrum from that study at T_e = 1000 K and log g= 5.0 is displayed in Figure 3.

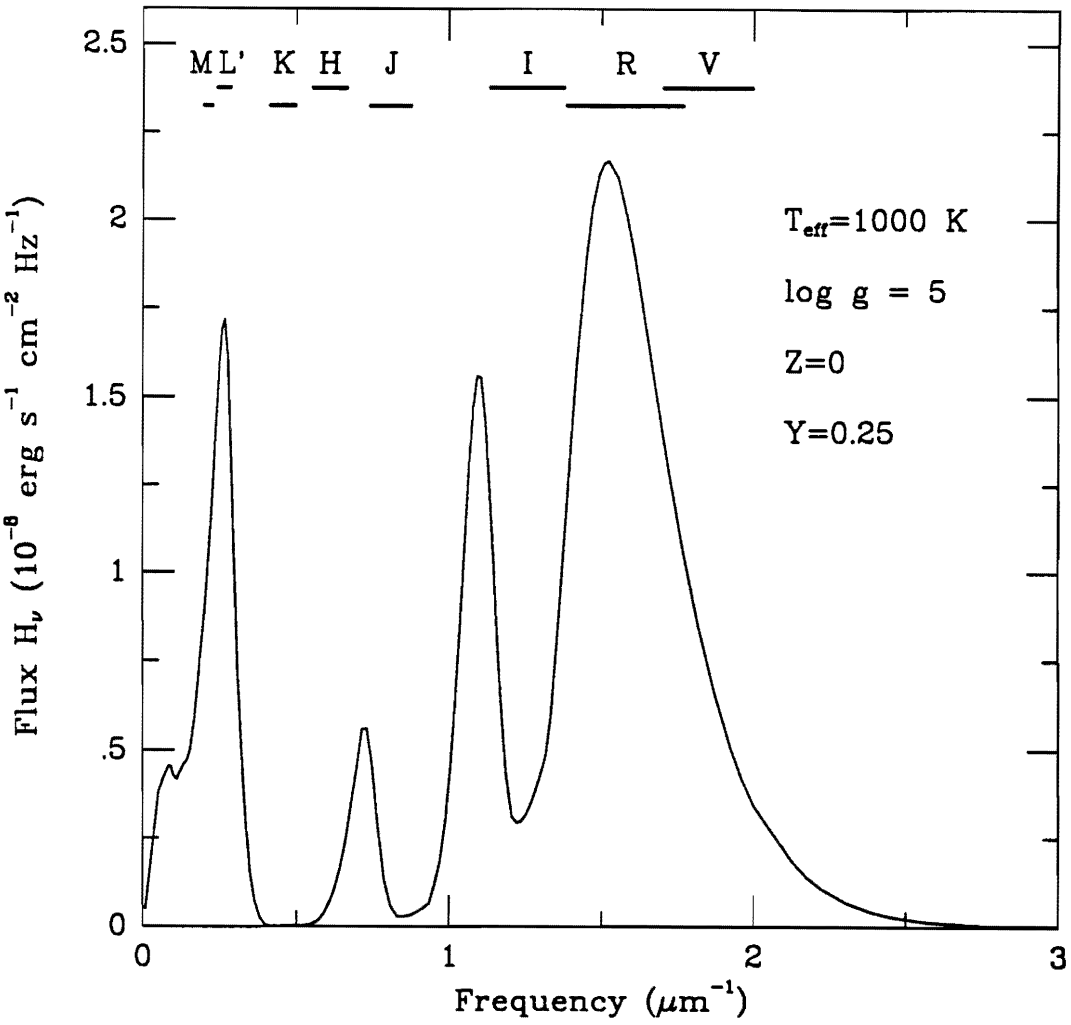

Figure 3. A spectrum from a theoretical zero-metallicity atmosphere with $T_{\rm eff}$ = 1000 K and $\log g$ = 5, taken from Saumon *et al.*[24]

At low effective temperatures, molecular hydrogen dominates the atmospheric composition and the collision-induced H_2 opacity ***strongly affects the spectrum***, as can be seen in Figure 3 for T_e = 1000K. Each trough in the emergent infrared flux corresponds to an absorption band of H_2. For T_e < 3000 K, the opacity is dominated by collision-induced H_2 absorption and by H_2 Rayleigh scattering. At higher temperatures, H^- takes precedence over Rayleigh scattering. The resulting spectrum bears no resemblance to a blackbody flux distribution when H_2 absorption

dominates, and the spectrum becomes *bluer at lower* T_e and when the gravity is increased, as expected from the temperature and density dependence of the H_2 absorption coefficient. We note significant differences in the infrared ($\nu < 1\ \mu m^{-1}$ flux with the very low-metallicity models of Allard[22] which are due to our use of updated cross-sections for the H_2 absorption.

There is a dramatic difference between grey and nongrey structures, particularly in the value of the boundary temperature. This is caused by strong departures of the opacity from greyness once collision-induced H_2 opacity becomes important. This opacity source forces the top of the convection zone to rise higher in the atmosphere than in the grey case, leading to a lower boundary temperature.

If we neglect the minute amounts of elements heavier than helium produced during the primordial nucleosynthesis, zero-metallicity models would describe the very first generation of stars, the so-called Population III stars. The mass function of this stellar population could extend down to the M dwarf range since collapsing clouds might fragment into low mass stars even in the absence of heavy elements.[57] Burrows *et al.*[21] shows that $Z = 0$ brown dwarfs are all extremely faint and essentially undetectable after 10^{10} yr of cooling, with $L/L_\odot \lesssim 10^{-6}$. This is a consequence of their transparent atmospheres which allow energy to escape more freely. On the other hand, if M dwarfs of zero metallicity formed in the distant past, they have remained virtually unchanged to this day.

Zero-metallicity brown dwarfs serve as yet another interesting limiting case. As pointed out by Stevenson,[58] cool low-mass brown dwarfs can potentially differentiate their metals into a central core, by virtue of the limited solubility of $Z > 2$ elements in metallic hydrogen under brown-dwarf physical conditions. Although such elements do not contribute significantly to the energy balance, they contribute in a major way to the evolutionary timescale and emergent spectra, an effect which we have now bounded. We have established that this effect alone is unlikely to produce a pure zero-metallicity brown dwarf atmosphere within a Hubble time, yet some abundant elements with larger values of Z (such as silicon, vanadium, and iron) may well vanish from the atmospheres of very old brown dwarfs with masses less than about 0.06 $M_\odot$, with repercussions for the cooling times.

However, searches for Population III objects have to date been fruitless at all masses. High velocity, metal-poor subdwarfs in the solar neighborhood are seen at masses down to 0.1 solar masses, based on observations of Monet *et al.*,[59] and models of D'Antona.[13] These assume a metallicity of 0.005 times solar (Population II). An interesting issue is whether the use of pure hydrogen-helium models significantly changes the interpretation of the observations of Monet *et al.*,[59] in terms of the masses. Determining the degree of sensitivity of model properties at low metallicity is required for determining the IMF of halo subdwarfs from observations.

Interpretation of surveys of field halo populations[60] are hampered by the fair range of metallicity expected for such objects. The halo field star results down to 0.14 solar masses are consistent with a Salpeter mass function;[60] extrapolating downward in mass would allow low mass brown dwarfs to dominate the dark matter content of the galaxy. Thus, while Population III objects may be absent from

the halo, use of our metal-free models provides an important sensitivity test in the interpretation of metal-poor subdwarfs, using the most up-to-date continuum opacities available.

4. Dark Matter in the Galactic Halo

The recent observation of microlensing events of LMC giants by halo objects (Livermore,[61] EROS[62]) and by what appear to be bulge M dwarfs[63] has sparked speculation about the cool star and/or brown dwarf content of the halo and bulge.

A microlensing event occurs when the relative transverse motion of the star and the lens brings the star near and into the so-called Einstein radius which is proportional to the square root of the lens mass and an "effective" lens distance.[64,65] The deeper the star penetrates the Einstein radius, the larger the amplification. The duration of the event is equal to the ratio of the Einstein radius to the relative transverse velocity, V_T. From the two parameters of amplification and duration, properties of the lens can be inferred. However, without knowledge of the lens distance (D) and the transverse velocity, the system is underdetermined. A lens mass can be quoted only after D and V_T are guessed and with large error bars. Without D and V_T for each event, the question of whether MACHOs are the halo can be answered only with a halo model, Monte Carlos, and many events to provide respectable statistics. The MACHO collaboration has about 10^7 two-color light curves from which they have identified four candidate microlensing events with maximum amplification (A) from 7.1 (their "gold-plated" event) to ~1.5. They derive best-fit lens masses of 0.02 $M_\odot$, 0.04 $M_\odot$, 0.06 $M_\odot$ and 0.13 $M_\odot$, with large error bars. The EROS collaboration, with slightly lower throughput, have identified two candidate events with A of ~2.5 and 3.0. They also have seen the MACHO collaboration's gold-plated candidate. Neither collaboration quotes the detection efficiencies of their survey, without which an estimate of the MACHO fraction of the halo (f_m) can not be made. f_m's from 5% to 100% are still possible. The average duration for the candidates of both collaborations is near one month. Such a short duration, with a V_T of 300 km/s and a D of 10 kpc, implies that all the candidate lenses have Einstein radii near 1 A.U. and are indeed of low mass ($\leq 0.1 M_\odot$). They are not white dwarfs, neutron stars, or black holes.

The question that naturally arises is whether such a population could have been detected already or can now be detected in a dedicated search. At a distance of ~ 10 kpc and with a transverse velocity of ~ 200 km/s the lens would be moving only at $0.1''$/25 years. Without knowing the metallicity and mass of the lens star, we can't predict its brightness. However, we can present estimates of its band emissions under a variety of reasonable assumptions. Table 2 lists estimates of the absolute magnitudes in various photometric bands of, a) the edge solar metallicity M dwarf ($0.077 M_\odot$), b) the edge zero-metallicity M dwarf ($0.092\ M_\odot$), c) an edge subdwarf, and d) a $0.08 M_\odot$, 10^{10} year old zero-metallicity brown dwarf. The data of Monet *et al.*,[59] Tinney,[2] Dahn *et al.*,[66] Bessell,[67] and the theoretical work of Saumon *et al.*[24] and Burrows *et al.*[21] were used to compile these estimates, good to perhaps a few

tenths of a magnitude. This table is an updated version of one found in Burrows *et al.*[68] As Table 2 hints, low metallicity M dwarfs are "bright", solar metallicity brown dwarfs are dim, and zero-metallicity brown dwarfs are exceedingly dim and anomolously blue.

Table 2
Approximate Magnitudes At the Main Sequence Edge*

	a) $M = 0.077M_\odot$ $Z = Z_\odot$	b) Edge Subdwarf	c) $M = 0.092M_\odot$ $Z = 0.0$	d) $M = 0.08M_\odot$ $Z = 0.0$ (10^{10} years)
M_V	19.5	14.5	12.8	19.4
M_R	17.3	14.0	12.0	18.4
M_I	15	11.8	11.2	19.6
M_K	10.5	9.7	11.1	24.4
M_B	21.7	16.6	14.0	22.0
$M_{\rm Bol}$	15.3	12.1	12.2	19.5

* Numbers are good to a few tenths of a magnitude and are derived or extrapolated from theoretical calculations or observations found in D.G. Monet *et al.*,[59]. Tinney,[2] D. Saumon *et al.*,[24] M.S. Bessel,[67] C. Dahn, J. Liebert, and H. Harris,[69] and BHSL.

One thing that Table 2 tells us is that if the limiting magnitudes of a search in B, V, R, I, and K are 28, 27, 26, 25, and 21, respectively, though K and I are the preferred bands for searches for solar-metallicity dwarfs, R, I, and V are the preferred bands at the lower metallicities. This fact is relevant for halo MACHO searches, since the dark matter of the halo must be old and primitive. However, if, as is suggested by the microlensing surveys, MACHOs are brown dwarfs, they will be very difficult (but not impossible in the solar neighborhood) to detect at any metallicity.

At 10 kpc, a solar-metallicity edge M dwarf has a V magnitude of 34.5 and a K magnitude of 26, while a zero-metallicity edge M dwarf has a V magnitude of 28 and an R magnitude of 27. A zero-metallicity brown dwarf has a V magnitude of 34.4 and a K magnitude of 39.4! Clearly, a brown dwarf halo population of whatever metallicity would be very difficult to detect photometrically. A solar-metallicity M dwarf population would also be difficult (but easier) to acquire. However, a subdwarf or zero-metallicity M dwarf population would be *many* magnitudes brighter from V through I and should already have been detected (if there in abundance) in deep pencil-beam surveys.[70] As a case in point, Tyson[71] observed in B, R, and I to completeness limits of 27.7(B), 26.6(R), and 25.1(I) in 10 fields, each $\sim$11 square arcmins in size. If the dark matter were made up of zero-metallicity brown dwarfs and M dwarfs with a continuous Salpeter mass function extending from $0.01M_\odot$, Tyson[71] should have seen in R a *thousand* M dwarfs per field. If this population were subdwarfs and they extended into the dark matter halo to provide the "dark" matter, Tyson[71] would have seen a *hundred* of them. Instead, he has identified no such population of stars, while detecting more than one thousand galaxies per field! (see, however, Gould[72]) In order for the dark matter halo to be made up of cool

stars, they must be brown dwarfs, not M dwarfs and the halo mass function must be discontinuous. Solar metallicity M dwarfs at the requisite halo density would have been identified in the solar neighborhood by their kinematics and have not been.[59] Furthermore, a subdwarf or zero-metallicity halo population sufficient to make up the halo dark matter would have been detected in the local subdwarf sample with about one hundred times the actual observed number density.[66]

5. Conclusion

Since new theoretical spectra and colors will soon be available and infrared technology and surveys are continuing their explosive advance, brown dwarf studies are rapidly joining the other more established branches of stellar astronomy. These substellar objects bridge the realms of planets and stars, may provide the missing mass of the halo, and reside on one of the last frontiers of the stellar astronomy.

6. Acknowledgments

The authors wish to thank Jim Liebert, Pat Boeshaar, Davy Kirkpatrick, and Roger Angel for useful conversations and advice. They would also like to acknowledge support through NSF grants AST92-17322 and AST93-18970 and NASA grant NAGW-2145. D. Saumon acknowledges the support of a Hubble Fellowship.

7. References

1. Kroupa, P., Tout, C.A., and Gilmore, G., *MNRAS* **262** (1993) 545.
2. Tinney, C., *Ap. J.* **414** (1993) 279.
3. Henry, T.J., Ph.D. Thesis, University of Arizona, (1991).
4. Kirkpatrick, J.D., Henry, T.J., and McCarthy, D., *Ap. J. Supp.* **77** (1991) 417.
5. Latham, D.W., Mazeh, T., Stefanik, R.P., Mayor, M., and Burki, G., *Nature* **339** (1989) 38.
6. Schneider, D.P., Greenstein, J.L., Schmidt, M., and Gunn, J.E., *Astrophys. J.* **102** (1991) 1180.
7. Becklin, E.E. and Zuckerman, B., *Nature* **336** (1988) 656.
8. Tinney, C., Mould, J. R., and Reid, I. N., *ApJ* **396** (1993) 173.
9. Comeron, F., Rieke, G., Burrows, A., and Rieke M., *Ap. J.* **416** (1993) 185.
10. Stauffer, J., Hamilton, D., Probst, R., Rieke, G., and Mateo, M., *Ap. J. Lett.* **344** (1989) L21.
11. Burrows, A. and Liebert, J., *Rev. Mod. Phys.* **65** (1993) 301.
12. D'Antona, F. and Mazzitelli, I., *Ap. J.* **296** (1985) 502.
13. D'Antona, F., *Ap. J.* **320** (1987) 653.
14. Nelson, L.A., Rappaport, S.A., and Joss, P.C., *Ap. J.* **304** (1986a) 231.
15. Nelson, L.A., Rappaport, S.A., and Joss, P.C., *Ap. J.* **311** (1986b) 226.
16. Nelson, L.A., Joss, P.C., and Rappaport, S.A., *Ap. J.* **404** (1993) 723.

17. Stringfellow, G.S., in *Astrophysics of Brown Dwarfs,* edited by M.C. Kafatos, R.S. Harrington, and S.P. Maran (Cambridge Univ. Press), p. 190., (1986).
18. Stringfellow, G.S., *Ap. J. Lett.* **375** (1991) L21.
19. Dorman, B., Nelson, L.A., and Chau, W.Y., *Ap. J.* **342** (1989) 1003.
20. Burrows, A., Hubbard, W.B., and Lunine, J.I., *Ap. J.* **345** (1989) 939 (BHL).
21. Burrows, A., Hubbard, W.B., Saumon, D., and Lunine, J.I., *Ap. J.* **406** (1993) 158 (BHSL).
22. Allard, F., Ph.D. Thesis, Heidelberg, (1990).
23. Allard, F. *et al.*, *Ap. J.* **426** (1994) L39.
24. Saumon, D., Bergeron, P., Lunine, J.I., Hubbard, W.B., and Burrows, A.B., *Ap. J.* **424** (1994) 333.
25. Kui, R., Ph.D. Thesis, Mt. Strombo University, (1991).
26. Kirkpatrick, J.D., Henry, T.J., and Liebert, J., *Ap. J.* in press, (1993).
27. Kumar, S., *Ap. J.* **137** (1963) 1121.
28. Grossman, A.S., Hayes, D., and Graboske, H.C., *AA* **30** (1974) 95.
29. Vandenberg, D.A., Hartwick, F.D.A., Dawson, P., and Alexander, D.R., *Ap. J.* **266** (1983) 747.
30. Wigner, E. and Huntington, H. B., *J. Chem. Phys.* **3** (1935) 764.
31. Mao, H.K., Hemley, R.J., and Hanfland, M., *Phys. Rev. Lett.* **65** (1990) 484.
32. Mao, H.K. and Hemley, R.J., *Science* **244** (1989) 1462.
33. Van Horn, H.M., *Science* **252** (1991) 384.
34. Stevenson, D. J., *Phys. Lett.* **58A** (1976) 282.
35. Stevenson, D. J., *Ann. Rev. Astron. Astrophys.* **29** (1991) 163.
36. DeWitt, H.E. and Hubbard, W.B., *Ap. J.* **205** (1976) 295.
37. Slattery, W.L., Doolen, G.D., and DeWitt, H.E., *Phys. Rev.* **A26** (1982) 2255.
38. Marley, M.S. and Hubbard, W.B., *Icarus* **73** (1988) 536 (MH).
39. Magni, G. and Mazzitelli, I., *AA* **72** (1979) 134.
40. Stringfellow, G.S., DeWitt, H.E., and Slattery, W.L., *Phys. Rev.* **41A** (1990) 1105.
41. Mestel, L. and Ruderman, M. A., *M.N.R.A.S* **136** (1967) 27.
42. Saumon, D. and Chabrier, G., *Phys. Rev. Lett.* **62** (1989) 2397 (SC).
43. Saumon, D. and Chabrier, G., *Phys. Rev.* **A46** (1992) 2084 (SC).
44. Saumon, D., Ph.D. thesis, University of Rochester, (1990).
45. Fontaine, G., Graboske, H.C., Jr., and Van Horn, H.M., *Ap. J.* **35** (1977) 293.
46. Däppen, W., Mihalas, D., Hummer, D.G. and Milahas, B.W., *Ap. J.* **332** (1988) 261.
47. Eggleton, P. P., Faulkner, J., and Flannery, B. P., *A&A* **23** (1973) 325.
48. Berriman, G. and Reid, N., *M.N.R.A.S* **227** (1987) 315.
49. Liebert, J. and Probst, R. G., *Ann. Rev. Astron. Astrophys.* **25** (1987) 473.
50. Lunine, J.I., Hubbard, W.B., Burrows, A., Wang, V.P., and Garlow, K., *Ap. J.* **338** (1989) 314.
51. Lenzuni, P., Chernoff, D., and Salpeter, E.E., *Ap. J. Suppl.* **76** (1991) 759.
52. Bergeron, P., Wesemael, F., and Fontaine, G., *Ap. J.* **367** (1990) 253.

53. Fowler, W. A., Caughlan, G. R., and Zimmerman, B. A., *Ann. Rev. Astron. Astrophys.* **13** (1975) 69.
54. Graboske, H. C., DeWitt, H. E., Grossman, A. S., and Cooper, M. S., *Ap. J.* **181** (1973) 457.
55. Bryja, C. *et al.*, *Ap. J. Lett.* **388** (1992) L23.
56. Hubbard, W.B., Burrows, A., and Lunine, J.I., *Ap. J. Lett.* **358** (1990) L53.
57. Palla, F., Salpeter, E.E., and Stahler, S.W., *Ap. J.* **271** (1983) 632.
58. Stevenson, D.J., in *Astrophysics of Brown Dwarfs*, edited by M. C. Kafatos, R. S. Harrington, and S. P. Maran (Cambridge Univ. Press),p. 218, (1986).
59. Monet, D.G. *et al.*, *Astron. J.* **103** (1992) 638.
here
60. Richer, H. B. and Fahlman, G.G., *Nature* **358** (1992) 383.
61. Alcock, C. *et al.*, *Nature* **365** (1993) 621.
62. Aubourg, E. *et al.*, *Nature* **365** (1993) 623.
63. Udalski, A., *et al.*, *Acta Astronomica* **43** (1993) 289.
64. Griest, K., *Ap. J.* **366** (1991) 412.
65. Paczynski, B., *Ap. J.* **304** (1986) 1.
66. Dahn, C.C., Liebert, J., Harris, H.C., and Boeshaar, P.C., in preparation, (1994).
67. Bessell, M.S., *Astron. J.* **101** (1991) 662.
68. Burrows, A., Hubbard, W.B., and Lunine, J.I., to appear in the Proceedings of the Eighth Cambridge Workshop on Cool Stars, Stellar Systems, and the Sun, ed. J.-P. Caillault, (1994).
69. Dahn, C.C., Liebert, J., and Harris, H., in preparation, (1994).
70. Bahcall, J. N. *et al.*, *Ap. J. Lett.*, in press, (1994).
71. Tyson, A., *Astron. J.* **96** (1988) 1.
72. Gould, A., *Ap. J.* **386** (1992) L5.